

Nonlinear Life-Extending Control of a Rocket Engine

Carl F. Lorenzo*

NASA John Glenn Research Center at Lewis Field,
Cleveland, Ohio 44135

and

Michael S. Holmes† and Asok Ray‡
The Pennsylvania State University,
University Park, Pennsylvania 16802

I. Introduction

A ROCKET engine has a number of critical components that operate close to mechanical design limits. These components often typify behavior of the remaining components and hence are indicators of the effective service life of a reusable rocket engine. Fatigue damage in the turbine blades is one of the most serious causes for engine failure. This Note focuses on the conceptual development of a nonlinear life-extending control system for rocket engines via damage mitigation in both the fuel (H_2) and oxidizer (O_2) turbine blades.

The fundamental concept of life-extending control (LEC) was introduced by Lorenzo and Merrill.¹ Subsequently, a growing body of literature has emerged for feedforward^{2,3} and feedback⁴ control of rocket engines for life extension. Whereas the LEC technology was developed initially for rocket engines, it has broad applications for other systems such as fossil-fueled power plants⁵ and mechanical structures,⁶ where both dynamic performance and structural durability are critical issues.

The design approach presented in this Note is different from previous work in the sense that this approach allows adaptation of the LEC feature to augment a conventional performance controller of a rocket engine. Unlike the previously reported design approaches,^{2,3,5} the proposed technique does not require an optimal feedforward control sequence, which is sensitive to plant modeling uncertainties and variations in the initial conditions. Furthermore, for other control applications such as military aircraft, the life extension feature of the control system can be activated or deactivated at the operator's discretion.

II. Structure of the Life-Extending Control (LEC) System

The reusable rocket engine under consideration is functionally similar to the space shuttle main engine. A thermo-fluid-dynamic model⁷ of the rocket engine has been formulated for control systems synthesis based on its functional characteristics. The plant model has 18 state variables, 2 control inputs, and 2 controlled outputs. The oxygen flow into the two preburners is independently controlled by the respective servo-valves. The plant outputs of interest are the main thrust chamber hot gas pressure and oxygen/hydrogen (O_2/H_2) mixture ratio that are closely related to engine performance in terms of specific impulse, thrust, and combustion temperature.⁷

Figure 1 shows the architecture of the proposed two-tier LEC system consisting of two loops: (linear robust) performance control as the inner loop and (nonlinear) damage control as the outer loop. Both inner-loop and outer-loop controllers are designed in discrete time for direct implementation on the control computer(s). For rocket engine control the inner-loop controller is designed using H_∞ -based μ synthesis to ensure stability and performance robustness independent of the outer-loop damage controller. The combination of plant dynamics and the performance controller in the inner loop becomes

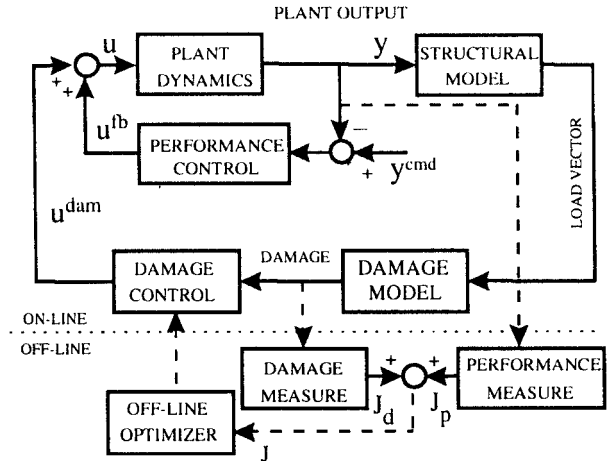


Fig. 1 Schematic diagram of on-line LEC and off-line optimization systems.

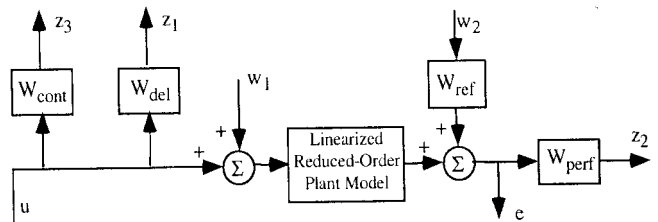


Fig. 2 Generalized plant model for linear robust controller synthesis.

the augmented plant for designing the outer-loop damage controller that includes the nonlinear damage characteristics of structural materials. Optimization of the outer-loop controller parameters includes this augmented model. This is an alternative approach to the fuzzy damage controller design proposed by Holmes and Ray.⁴

The essential elements of the damage controller in the outer loop are the following: 1) a structural model² that uses appropriate plant outputs to estimate the load conditions (e.g., stresses at the critical locations of turbine blades); 2) a nonlinear model of damage rate and accumulation that is excited by the load conditions; and 3) the damage controller, which is designed to reduce the damage rate and accumulation at the critical points, specifically under transient operations when the time-dependent load on the stressed structure is controllable. Whereas the inner-loop performance controller is valid in response to any exogenous inputs within allowable bounds, the outer-loop damage controller is designed for specific operating conditions. The rationale for this restriction is that the damage process is highly nonlinear, and it may not be possible to achieve a damage controller for arbitrary inputs without a significant loss of performance.

III. Design of the Inner-Loop Linear Performance Controller

This section presents the synthesis of a sampled-data performance controller in the inner loop by using the H_∞ (or induced L_2 norm to L_2 norm) technique that minimizes the worst-case gain between the energy of the exogenous inputs and the energy of the regulated outputs of a generalized plant shown in Fig. 2. The performance controller needs to have very good low-frequency disturbance rejection capabilities to prevent the damage controller output u^{dam} from causing a long settling time of the plant outputs. We have adopted the sampled-data controller design procedure of Bamieh and Pearson⁸ that has subsequently been incorporated as the function `sdhfsyn` in the MATLAB[®] mutools toolbox.⁹

Figure 2 shows the setup used for synthesis of an induced L_2 norm controller based on the rocket engine model with two inputs, fuel preburner oxidizer valve position and oxidizer preburner oxidizer valve position, and two outputs, main thrust chamber hot-gas pressure and O_2/H_2 mixture ratio. The plant model is obtained by first linearizing the 18-state nonlinear model of the rocket engine⁷

Received 22 July 1999; revision received 23 January 2000; accepted for publication 9 February 2000. Copyright © 2000 by the American Institute of Aeronautics and Astronautics, Inc. All rights reserved.

*Distinguished Research Associate, Instrumentation and Control Technology Division, 21000 Brookpark Road.

†Graduate Research Assistant, Mechanical Engineering Department.

‡Professor of Mechanical Engineering, Associate Fellow AIAA.

at a combustion pressure of 2550 psi (0.370 MPa) and an O_2/H_2 ratio of 6.02. The nominal operating point at pressure 2550 psi (0.370 MPa) and O_2/H_2 mixture ratio 6.02 is chosen for linearization because this controller is designed to be functional in the range 2100 psi (0.305 MPa) to 3000 psi (0.370 MPa) with a constant O_2/H_2 mixture ratio 6.02. After linearization the 18-state linear model is reduced to a 13-state linear model for the controller design via Hankel model order reduction.¹⁰ An examination of Bode plots reveals that reducing the 18-state model to a 13-state model does not significantly alter the input-output characteristics of the original model. Because the induced L_2 -norm controller synthesis procedure being used here requires a strictly proper generalized plant model, the problem of a nonzero D matrix is circumvented by filtering the outputs of the controller by a first-order filter with a high-frequency pole at 10^4 rad/s:

$$W_{\text{filter}}(s) = 10^4 / (s + 10^4) \quad (1)$$

The input multiplicative configuration is chosen to represent the plant model uncertainties caused by parametric errors and unmodeled high-frequency dynamics. The sampler and zero-order hold associated with the controller are implicit in the setup used for robust stability as shown in Fig. 2, where each of the two components of the frequency-dependent disturbance weight W_{del} is chosen to be

$$W_{\text{del}}(s) = (s + 1) / (s + 10) \quad (2)$$

which implies that the amount of plant uncertainty is estimated as being approximately 10% at low frequencies and 100% at high frequencies. The uncertainty model is constructed based on the assumptions of the rocket engine design and operation and can be updated as additional analytical or experimental data become available. Because the plant model is validated with steady-state design data, it is more accurate in the low-frequency range. The plant model is a finite dimensional lumped-parameter representation that may not capture the dynamics of high-frequency modes. This leads to the presence of a larger amount of uncertainty in the high-frequency region of the model as compared to the uncertainty at low frequencies.

The frequency-dependent performance weight W_{perf} consists of two components: 1) W_{press} , which penalizes the tracking error of combustion chamber pressure, and 2) W_{O_2/H_2} , which penalizes the tracking error of the O_2/H_2 ratio. The frequency-dependent control signal weight W_{cont} consists of two components: 1) W_{H_2} to penalize the fuel preburner oxidizer valve motion, and 2) W_{O_2} to penalize the oxidizer preburner oxidizer valve motion. The objectives of these frequency-dependent weights are the following: 1) prevention of large oscillations in the feedback control signal to avoid valve saturation and 2) reduction of valve wear and tear caused by high-frequency movements.

The parameters of both performance weights and control weights are initially selected based on the control system performance requirements and the knowledge of the plant dynamics. Subsequently, these parameters are fine tuned using the time-domain responses of the simulation experiments. For this rocket engine controller design the performance weights are

$$W_{\text{press}}(s) = 4 \left(\frac{s + 1.75}{s + 1} \right), \quad W_{O_2/H_2}(s) = 4000 \left(\frac{s + 0.5}{s + 0.1} \right) \quad (3)$$

The control weight for both valves is

$$W_{H_2}(s) = W_{O_2}(s) = 1200[(s + 10)/(s + 100)] \quad (4)$$

Each of the two components of the frequency-dependent reference signal weight W_{ref} in Fig. 2 is chosen to be

$$W_{\text{ref}}(s) = 0.5 / (s + 0.5) \quad (5)$$

Following the generalized plant model in Fig. 2, a sampled-data controller is designed, which is optimal in the induced L_2 -norm sense. As guaranteed by the design method employed, the controller has 23 states, which is the same as the number of states in the generalized plant model that consists of the reduced-order plant model (13 states), the control signal filters (2 states), the uncertainty weighting matrix (2 states), the performance weighting matrix (2 states), the

reference-signal weighting matrix (2 states), and the control-signal weighting matrix (2 states). Reducing the order of the sampled-data controller from 23 states to 15 states causes no significant change in the controller dynamics from an input/output point of view. Furthermore, this reduction causes no noticeable difference in the simulation results.

IV. Design of the Outer-Loop Nonlinear Damage Controller

Damage modeling is a critically important aspect of LEC design. The damage model has a state-variable structure that is suitable for controller design as well for implementation of the controller itself. Because the model is embedded in the damage control loop, it should be mathematically consistent and computationally simple while adequately representing the damage characteristics for the purposes of optimization and control. The implication is that the absolute level of the damage rate may not be so important as the structure of the damage equation, i.e., the nonlinearities must be properly described to realize the relative gain or loss in damage under different control actions. Details of the damage modeling method are reported by Lorenzo¹¹ and Ray et al.²

As seen in Fig. 1, the outer damage control loop is a cascaded combination of a structural model and a fatigue damage model of the turbine blades and a linear dynamic filter acting as the damage controller. The controller parameters are optimized to reduce the damage rate and accumulation at the critical points (i.e., fuel and oxidizer turbine blades) specifically under transient operations where the time-dependent load on the stressed structure is controllable. The nonlinear damage model is a simplified representation of the material behavior so that it can be incorporated in the outer control loop for real-time execution.

The parameters of the linear part of the damage controller are identified by minimizing a cost functional using nonlinear programming.¹² The cost functional is numerically evaluated as a function of the current values of damage controller parameters that are chosen by the optimization routine at each iteration. Because the design of damage controllers is directly based on the maneuver used in the optimization process, such maneuvers should be chosen to be representative of relevant plant operations. The resulting damage controller is then validated by simulation experiments on other maneuvers that the plant is expected to perform with this damage controller. The controller design is largely application specific and relies on a certain class of rocket engine operations as discussed next.

The design of the damage controller is based on a ramp-up operation of the main thrust chamber pressure from a level of 2700 psi (0.392 MPa) to 3000 psi (0.435 MPa) at a rate of 3000 psi/s (0.435 MPa/s), followed by a steady state at the final 3000 psi (0.435 MPa) pressure for 500 ms. The O_2/H_2 mixture ratio for this operation is desired to be kept constant at a value of 6.02. The generated outputs of simulation experiments at sampling intervals of $T = 2$ ms are the chamber pressure, the O_2/H_2 mixture ratio, and the accumulated damage and damage rate in the O_2 and H_2 turbine blades. Thus, a total of $N + 1$ samples are generated for each trajectory over a duration of $2N$ ms. The data set for each trajectory is used to calculate the total cost functional J that includes the effects of both dynamic performance cost J_p of reference signal tracking and damage cost J_d :

$$J = J_p + J_d \quad (6)$$

where J_p is obtained as a combination of the penalties on the tracking errors of the main thrust chamber hot-gas pressure and the O_2/H_2 mixture ratio and J_d is obtained as a combination of the penalties on fatigue damage rate and accumulation in the O_2 and H_2 turbine blades. Details on construction of the cost functionals are reported by Lorenzo et al.¹³

The linear part of the nonlinear damage controller was initially structured to have a canonical form with 15 states ($n = 15$), 2 actuator inputs ($m = 2$), and 2 sensor outputs ($p = 2$). It is found from simulation results that after designing the 15-state damage controller reducing the number of controller states to 5 via Hankel model order reduction does not significantly change the input/output characteristics of the controller.

The inner control loop is guaranteed to be robustly stable with respect to the specified uncertainty description. The damage control signal u^{dam} in Fig. 1 acts as an exogenous disturbance to the inner loop. However, outer-loop stability is not guaranteed by off-line optimization for parameter identification. If the outer-loop controller is given limited authority, i.e., if bounds are imposed on u^{dam} , it will be unable to destabilize the inner control loop, and the system response remains bounded although this does not establish stability in the sense of Lyapunov. For example, there is no guarantee that phenomena like limit cycling of the control signals will not occur. Further research is needed to explore nonlinear controller synthesis techniques⁴ to satisfy simultaneously the requirements of stability and performance in nonlinear life-extending control systems. However, from the perspectives of rocket engine control, outer-loop stability is not problematic because the total flight time is very limited (e.g., ~ 420 s). Extensive simulation experiments over this finite-time horizon of active engine operation show that the two-tier control system is stable without imposition of any bounds on the damage control signal u^{dam} .

V. Simulation Results and Discussion

Simulation experiments are based on the 18-state rocket engine model coupled with the 15-state reduced-order performance controller in the inner loop and 5-state reduced-order damage controller in the outer loop. The damage controller is designed based on transients that take the chamber pressure from 2700 psi (0.392 MPa) to 3000 psi (0.435 MPa) at a rate of 3000 psi/s (0.435 MPa/s) as shown in Figs. 3–6. Each plot displays two cases: 1) with damage control, i.e., $u(k) = u^{\text{fb}}(k) + u^{\text{dam}}(k)$ and 2) without damage control, i.e., $u(k) = u^{\text{fb}}(k)$.

The chamber pressure trajectories for the two cases are compared in Fig. 3. The damage controller causes a slightly slower rise time, a longer settling time, and less overshoot in the chamber pressure transient. The damage controller also causes the O_2/H_2 ratio to deviate farther from the desired value of 6.02 than the case with no damage control as seen in Fig. 4. However, the mixture ratio settles to 6.02 at steady state and remains within acceptable bounds throughout the duration of the simulation for both cases. The damage accumulation plots for the first 1.0 s of the 2700 psi (0.392 MPa) to 3000 psi (0.435 MPa) simulation are shown in Figs. 5 and 6. Also, Table 1 summarizes the damage accumulation in O_2 and H_2 turbine

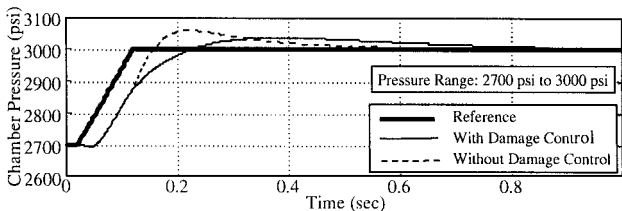


Fig. 3 Response of main combustion chamber hot-gas pressure.

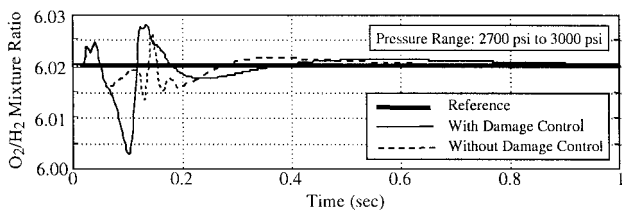


Fig. 4 Response of oxygen/hydrogen mixture ratio.

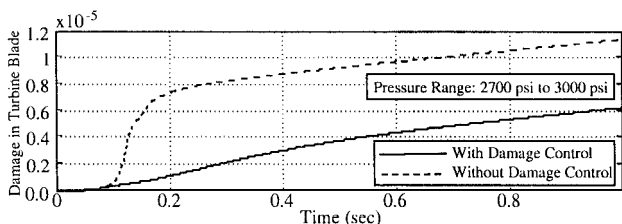


Fig. 5 Accumulated damage in hydrogen turbine blades.

Table 1 Accumulated damage (after 1.2 s) for 2100–3000 psi

Description	Without damage control	With damage control	Ratio
H_2 turbine blades	2.46×10^{-5}	9.61×10^{-6}	2.6
O_2 turbine blades	2.48×10^{-3}	7.01×10^{-5}	35.4

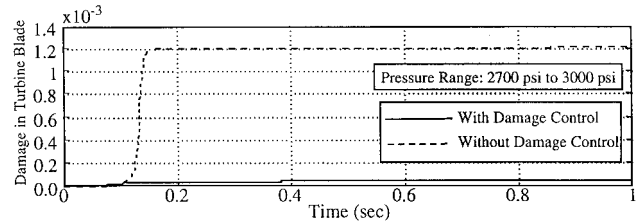


Fig. 6 Accumulated damage in oxygen turbine blades.

blades after the interval of 1.2 s for the two cases (i.e., with and without damage control) for the first 1.2 s of the 2100 psi (0.305 MPa) to 3000 psi (0.435 MPa) simulation. The modest loss of dynamic response of chamber pressure and the increased excursion in mixture ratio is the cost incurred for the substantially improved damage performance.

VI. Conclusions

This Note presents the conceptual development of a LEC system, where the objective is to achieve high performance and structural durability of the plant. The LEC is designed for a reusable rocket engine via damage mitigation in both the fuel (H_2) and oxidizer (O_2) turbines while achieving high performance for transient responses of the main thrust chamber pressure and the O_2/H_2 mixture ratio. The design procedure makes use of a combination of linear and nonlinear techniques and also allows adaptation of the life-extending controller module to augment a conventional performance controller of the rocket engine.

The two-tier architecture of the LEC system consists of a linear performance controller in the inner loop and a nonlinear damage controller in the outer loop. The high performance robust controller in the inner loop is designed using linear techniques (e.g., H_∞ -based μ synthesis) to achieve the required dynamic performance. The combination of rocket engine dynamics and the linear controller in the inner loop becomes the augmented plant for design of the nonlinear damage controller in the outer loop. The damage controller is realized as a cascaded combination of a nonlinear characterization of fatigue damage rate in the turbine blades and a linear dynamic filter. Parameters of the filter are optimized to reduce the damage rate and accumulation at the H_2 and O_2 turbine blades specifically under transient operations in which the time-dependent load on the stressed structure is controllable.

References

- Lorenzo, C. F., and Merrill, W. C., "An Intelligent Control System for Rocket Engines: Need, Vision, and Issues," *IEEE Control Systems Magazine*, Vol. 12, No. 1, 1991, pp. 42–46.
- Ray, A., Wu, M. K., Carpino, M., and Lorenzo, C. F., "Damage-Mitigating Control of Mechanical Systems: Parts I and II," *Journal of Dynamic Systems, Measurement and Control*, Vol. 116, No. 3, 1994, pp. 437–455.
- Dai, X., and Ray, A., "Damage-Mitigating Control of a Reusable Rocket Engine: Parts I and II," *Journal of Dynamic Systems, Measurement and Control*, Vol. 118, No. 3, 1996, pp. 401–415.
- Holmes, M., and Ray, A., "Fuzzy Damage Mitigating Control of Mechanical Structures," *Journal of Dynamic Systems, Measurement and Control*, Vol. 120, No. 2, 1998, pp. 249–256.
- Kallappa, P., Holmes, M. S., and Ray, A., "Life Extending Control of Fossil Power Plants for Structural Durability and Performance Enhancement," *Automatica*, Vol. 33, No. 6, 1997, pp. 1101–1118.
- Zhang, H., and Ray, A., "Robust Damage-Mitigating Control of Mechanical Structures: Experimental Validation on a Test Apparatus," *Journal of Dynamic Systems, Measurement, and Control*, Vol. 121, No. 3, 1999, pp. 377–385.
- Ray, A., and Dai, X., "Damage-Mitigating Control of a Reusable Rocket Engine," NASA CR 4640, Jan. 1995.

⁸Bamieh, B. A., and Pearson, J. B., Jr., "A General Framework for Linear Periodic Systems with Applications to H_∞ Sampled-Data Control," *IEEE Transactions on Automatic Control*, Vol. 37, No. 4, 1992, pp. 418–435.

⁹Balas, G. J., Doyle, J. C., Glover, K., Packard, A., and Smith, R., *μ -Analysis and Synthesis Toolbox*, MUSYN, Inc., and Math Works, Inc., Natick, MA, 1993.

¹⁰Zhou, K., Doyle, J. C., and Glover, K., *Robust and Optimal Control*, Prentice-Hall, Upper Saddle River, NJ, 1996, Chaps. 17–19.

¹¹Lorenzo, C. F., "Continuum Fatigue Damage Modeling for Use in Life Extending Control," NASA TM 106691, Aug. 1994.

¹²Gill, P. E., Murray, W., and Wright, M. H., *Practical Optimization*, Academic Press, London, 1981, Chap. 6.

¹³Lorenzo, C. F., Holmes, M. S., and Ray, A., "Design of Life Extending Controls Using Nonlinear Parameter Optimization," NASA TP 3700, April 1998.

¹⁴Khalil, H. K., *Nonlinear Systems*, 2nd ed., Prentice-Hall, Upper Saddle River, NJ, 1996, Chaps. 11–13.

Output Feedback Variable Structure Control for Uncertain Systems with Input Nonlinearities

Yi Shen,* Chunmei Liu,[†] and Hengzhang Hu[‡]
Harbin Institute of Technology,
150001 Harbin, People's Republic of China

Introduction

THE character of insensitivity to extraneous disturbance and internal parameter variations on a switching surface makes variable structure control (VSC) an effective method to control uncertain nonlinear dynamic systems. In theory, any control scheme that maintains its performance with the existence of uncertain factors should have a loop gain high enough. However, the inputs of a system are usually restricted by its physical structure and energy consumption, which also give the system inputs such nonlinear characters as saturation, deadzone, etc. The existence of nonlinear inputs is a source of degradation or, even worse, shows instability in the performance of the system.¹ Therefore, it is important to study the stability, robustness, and effective control of those systems with nonlinear inputs. In addition to nonlinear inputs, there are still plant uncertainties, such as identification inaccuracy, model truncation, plant parameter variation, etc. Therefore, more consideration is given to those systems with nonlinear inputs and uncertainties.

In Ref. 1, a new sliding mode control law based on the measurability of all of the system states is presented to ensure the global reaching condition of the sliding mode for uncertain systems with a series of nonlinearities. However, there often exist immeasurable states in a real system. Thus, we suggest a new law that requires only output information for output feedback VSC based on Ref. 1. An example is given to verify the sliding mode controller developed.

Problem Formulation

As in Ref. 1, an uncertain system with nonlinear input is described as

$$\dot{x}(t) = Ax(t) + B\Phi[u(t)] + f(x, p, t) \quad (1)$$

where $x(t) \in R^n$, $u(t) \in R^m$, $p(t) \in R^q$, and $f(t) \in R^s$ are the state variable, control input, uncertain parameter, and uncertain part of

the system, respectively. $A \in R^{n \times n}$ is the state matrix, $B \in R^{n \times m}$ the input matrix, and $\Phi(u) \in \Psi$ the nonlinear input function. It is also assumed that, for any initial condition $x(t_0) = x_0 \in R^n$, parameter $p(t) \in R^q$, and control input $u(t) \in R^m$, there exists a unique $x(t; x_0, p, u)$ that satisfies the system described in Eq. (1).

To delineate the nonlinear input function $\Phi(u)$, some of the definitions in Ref. 1 are given here.

Definition 1: Let diagonal matrix $\Gamma = \text{diag}[r_1, \dots, r_m] \in R^{m \times m}$ be positive definite.

Definition 2: The allowed series nonlinearities $\Phi(u)$ belong to the set

$$\Psi = \left\{ \Phi : R^m \rightarrow R^m; r_i u_i^2 \leq u_i \Phi_i(u), u_i \in R, \right. \\ \left. i = 1, \dots, m, u \in R^m \right\} \quad (2)$$

For the nonlinearity $\Phi(u) \in \Psi$, $\Phi(u)$ satisfies

$$u^T \Phi(u) \geq u^T \Gamma u \geq r u^T u \quad (3)$$

where $r = \min\{r_1, \dots, r_m\}$. For system (1) the following assumptions are made throughout.

Assumption 1: For all $i = 1, \dots, m$, if $u_i = 0$, then $\Phi_i(u) = 0$.

Assumption 2: For the uncertain system (1), matrix pair (A, B) is controllable, and the system is observable.

Assumption 3: For the uncertain part of the system, $f(x, p, t)$ meets the following matching condition:

$$f(x, p, t) = B\xi(x, p, t), \quad \|\xi(x, p, t)\| < k(y, t) \\ \forall (x, p, t) \in R^n \times R^p \times R \quad (4)$$

Design of Output Feedback Variable Structure Controller

Define the output of the system as $y = Cx$, $y \in R^r$. Assume that the system is observable and controllable, CB is full rank, and the open-loop system is minimum phase.² Define the linear switching surface as

$$S = Gy \quad (5)$$

where $G \in R^{m \times r}$. The sliding mode found from the equivalent control method is given by

$$\dot{x} = [A - B(GCB)^{-1}GCA]x \quad (6)$$

Switching surface G is assumed to have already been chosen such that GCB is invertible and Eq. (6) has desired characteristics (see Ref. 3). The equivalent control Φ_{eq} in the sliding mode can be derived from $\dot{S} = 0$:

$$\Phi_{\text{eq}} = -(GCB)^{-1}GC(AX + f) \quad (7)$$

Note that the equivalent control Φ_{eq} is a mathematical tool derived for the analysis of sliding motion rather than a real control law that can be generated in practical systems. The equivalent control generates an ideal sliding motion on the switching surface. It can be seen that uncertain systems possess the same properties in the sliding mode irrespective of whether or not there are input nonlinearities. Thereby, the switching surface can be selected in the same way as the design for systems with linear input.¹

Once a proper switching plane has been chosen, it is necessary to choose a discontinuous control law to guarantee the reaching condition of the sliding mode. The lemma in Ref. 1 is adopted here.

Lemma 1: For all allowable nonlinearities Φ_i belonging to set Ψ in Eq. (2), there exists a known continuous function $\rho(\cdot) : R_+ \rightarrow R_+$, $\rho(0) = 0$, $\rho(\eta) \geq 0$ for $\eta \geq 0$, such that, for all $u \in R^m$,

$$\rho(\|u\|) \leq u^T \Phi(u) \quad (8)$$

and there also exists a continuous function $\phi(\cdot) : R_+ \rightarrow R_+$, $\phi(0) = 0$, $\phi(\eta) \geq 0$, for $\eta \geq 0$, such that, for all $q \geq 0$,

$$\rho[\phi(q)] \geq q\phi(q) \quad (9)$$

Proof: Choose $\rho(\eta) = r\eta^2$, $r > 0$, then

$$\rho(\|u\|) = r\|u\|^2 = ru^T u \leq u^T \Phi(u) \quad (10)$$

Received 19 March 1999; revision received 25 October 1999; accepted for publication 26 October 1999. Copyright © 2000 by the American Institute of Aeronautics and Astronautics, Inc. All rights reserved.

*Professor, Department of Control Engineering, School of Astronautics; sy@ac411.hit.edu.cn.

[†]Doctoral candidate, Department of Control Engineering, School of Astronautics; rock@ac411.hit.edu.cn.

[‡]Professor, Department of Control Engineering, School of Astronautics.